J. of Basic Sciences, Cheju Nat'l Univ.
16(1), 11~17, 2003

기초과학연구 제주대학교
16(1), 11~17, 2003

Eikonal Phase Shift Analysis for $^{16}O + ^{16}O$ Elastic Scattering at E_{lab} = 704 MeV by Using a Tangential Velocity Correction

Yong Joo Kim
Department of Physics, Cheju National University

The refractive elastic scatterings of $^{16}O + ^{16}O$ system at E_{lab} = 704 MeV have been analyzed based on the Coulomb-modified eikonal phase shift using a tangential velocity at the distance of closest approach. The calculated result by introducing the tangential velocity satisfactorily reproduces experimental data concerning refractive pattern in the angular distributions of this system. The Fraunhöfer oscillations observed in the elastic angular distributions could be explained due to the interference between the near- and far-side amplitudes. The strongly real and weakly imaginary potentials are found to be essential to describe the refractive $^{16}O + ^{16}O$ elastic scatterings at E_{lab} = 704 MeV. The refractive part, dominated by the far-side component of the scattering amplitude, could be shown to be sensitive to the real heavy-ion optical potential at small radii.

I. INTROCUCTION

The data from the light heavy-ion systems at intermediate energies show in their angular distributions refractive features which are interpreted as the dominance of contributions from the far side of the scattering center. The refractive phenomena seen in the elastic scattering angular distributions for light heavy-ions provide a very valuable information on the heavy-ion optical potentials. Recent measurements [1-4] of elastic angular distributions for the $^{16}O + ^{16}O$ system at low and intermediate energies have attracted considerable interest, since they show a strongly refractive, with the elastic scattering pattern at large angles determined entirely by the far-side scattering. Furthermore, the weak absorption of the system is expected to help to determine the optical potential at small internuclear distances. Recently, there are several efforts [2-5] to describe the $^{16}O + ^{16}O$ elastic scattering. Bartnizky *et al.* [3] have measured the elastic scattering cross section for ^{16}O ions on ^{16}O targets with high accuracy over large angular ranges at incident energies from 250 to 704 MeV, and extracted the underlying scattering potentials using model-unrestricted analysis. The experimental data on this system at incident energies ranging from 124 to 1120 MeV have been analyzed [4] within the standard optical model, using either the phenomenological potential or that calculated within the double-folding model for the real part of the optical potential.

For many years, the eikonal approximation [6-8] has been found to be very effective approach to the description of the heavy-ions elastic scattering. There has been a great deal of effort [9-12] in describing elastic scattering processes between heavy ions within the framework of the eikonal approximation methods. The Glauber model with first- and second-order noneikonal corrections has been applied to elastic nuclear scattering at intermediate energies by Fäldt *et al.* [9]. Carstoiu and Lombard [10] investigated the limitations of the eikonal approximation in the low-energy regime for the calculation of total and total reaction cross sections. In our previous paper[13], we have presented the first- and second-order corrections to the zero-order eikonal phase shifts for heavy-ion elastic scatterings based on Coulomb trajectories of colliding nuclei and it has been applied satisfactorily to the $^{16}O + ^{40}Ca$ and $^{16}O + ^{90}Zr$ systems at E_{lab}=1503 MeV. The refractive elastic scatterings of $^{16}O + ^{16}O$ system at E_{lab}= 480, and 704 MeV are analyzed [14] within a framework of a second-order eikonal model.

The elastic cross section data of $^{16}O + ^{16}O$ scattering at E_{lab} = 704 MeV show the presence of refractive effect in the angular distributions. It is interesting to extend the Coulomb-modified eikonal model formalism to take into account a tangential relative velocity at the turning point of the corresponding classical trajectory and apply it to the refractive elastic $^{16}O + ^{16}O$ scattering at E_{lab} = 704 MeV. In this paper, we maintain the Coulomb-modified eikonal form of the phase

shift and try to replace the asymptotic velocity by tangential velocity at the point of closest approach. Some investigations on the major features of optical potential needed for fitting the observed data of this system are presented. In section II, we present the theory related with the eikonal formalism based on Coulomb trajectories, and tangential velocity correction at the distance of closest approach. Section III contains results and discussions. Finally, concluding remarks are presented in section IV.

II. THEORY

The elastic differential scattering cross section between two identical spinless nuclei is given by the following formula

$$\frac{d\sigma}{d\Omega} = |f(\theta) + f(\pi - \theta)|^2, \qquad (1)$$

where elastic scattering amplitude $f(\theta)$ is given by the equation

$$f(\theta) = f_{\rm R}(\theta) + \frac{1}{ik}\sum_{L=0}^{\infty}(L+\frac{1}{2})\exp(2i\sigma_L) \times(S_L^{\rm N}-1)P_L(\cos\theta). \qquad (2)$$

Here $f_{\rm R}(\theta)$ is the usual Rutherford scattering amplitude, k is the wave number and σ_L the Coulomb phase shifts. The nuclear S-matrix elements S_L^N can be expressed by the nuclear phase shifts δ_L

$$S_L^N = \exp(2i\delta_L). \qquad (3)$$

In this work, we use the eikonal phase shift based on the Coulomb trajectories of the colliding nuclei. If there is a single turning point in the radial Schrödinger equation, the WKB expression for the nuclear elastic phase shifts $\delta_L^{\rm WKB}$, taking into account the deflection effect due to Coulomb field, can be written as [7,15]

$$\delta_L^{\rm WKB} = \int_{r_t}^{\infty} k_L(r)\,dr - \int_{r_c}^{\infty} k_c(r)\,dr, \qquad (4)$$

where r_t and r_c are the turning points corresponding to the local wave numbers $k_L(r)$ and $k_c(r)$ given by

$$k_L(r) = k\Big[1-\Big(\frac{2\eta}{kr}+\frac{L(L+1)}{k^2r^2}+\frac{U(r)}{E}\Big)\Big]^{1/2}, \qquad (5)$$

and

$$k_c(r) = k\Big[1-\Big(\frac{2\eta}{kr}+\frac{L(L+1)}{k^2r^2}\Big)\Big]^{1/2}, \qquad (6)$$

where η is the Sommerfeld parameter, and $U(r)$ the nuclear potential. The distance of closest approach r_c is given by

$$r_c = \frac{1}{k}[\eta + [\eta^2 + L(L+1)]^{1/2}]. \qquad (7)$$

In the high-energy limit, we can consider the nuclear potential as a perturbation. Thus, the turning point r_t may be taken to be coincident with r_c and

$$k_L(r) - k_c(r) = k_c(r)\Big[1-\frac{2\mu U(r)}{\hbar^2k_c^2(r)}\Big]^{1/2} - k_c(r) \simeq -\frac{\mu U(r)}{\hbar^2 k_c(r)}. \qquad (8)$$

If we substitute Eq.(8) into Eq.(4) and rearrange the terms, we can find that the phase shift in terms of r_c instead of L, is given by

$$\delta_L(r_c) \simeq \int_{r_c}^{\infty}[k_L(r)-k_c(r)]dr = -\frac{\mu}{\hbar^2 k}\int_{r_c}^{\infty}\frac{rU(r)}{\sqrt{r^2-r_c^2}}dr. \qquad (9)$$

Furthermore, we have adopted a cylindrical coordinate system and decomposed the vector $\mathbf{r}$ as $\mathbf{r} = \mathbf{r}_c + z\hat{\mathbf{n}}$ where the z component of $\mathbf{r}$ lies along $\hat{\mathbf{n}}$ and $\mathbf{r}_c$ is perpendicular to $\hat{\mathbf{n}}$. We may, therefore, write Eq.(9) as

$$\delta(r_c) = -\frac{\mu}{\hbar^2 k}\int_0^{\infty}U(\sqrt{r_c^2+z^2})dz = -\frac{1}{\hbar v}\int_0^{\infty}U(\sqrt{r_c^2+z^2})dz, \qquad (10)$$

where v is the relative velocity of the two scattering partners at infinity. This is a phase shift for Coulomb-modified eikonal approximation.

In the semiclassical spirit, in order to assure the conservation of the angular momentum, one can change the asymptotic velocity

that is used to calculate the nuclear eikonal phase shift by the tangential velocity at the point of closest approach r_c,

$$v_c(b) = \frac{b}{r_c} v. \quad (11)$$

The Coulomb turning point correction in the eikonal phase shift of Eq.(10) then takes the form

$$\delta_L(r_c) = -\frac{1}{\hbar v_c} \int_0^\infty U(\sqrt{r_c^2 + z^2}) dz. \quad (12)$$

By taking $U(r)$ as the optical Woods-Saxon squared forms given by

$$U(r) = -\frac{V_0}{(1+e^{(r-R_v)/a_v})^2} - i\frac{W_0}{(1+e^{(r-R_w)/a_w})^2}, \quad (13)$$

with $R_{v,w} = r_{v,w}(A_1^{1/3} + A_2^{1/3})$, we can use the phase shift Eq.(12) in the general expression for the elastic scattering amplitude, Eqs.(1) and (2).

III. RESULTS AND DISCUSSIONS

The above Coulomb-modified eikonal phase shift with and without changing the asymptotic velocity at the point of closest approach r_c has been used to calculate the elastic differential cross sections for ^{16}O + ^{16}O system at E_{lab}= 704 MeV. Squared Woods-Saxon potential parameters were adjusted to obtain the least χ^2/N fit to the elastic scattering data. To increase the weight of data points at large angles which are especially sensitive to the strength and shape of the optical potential at small distances, we have assumed a 10 % uncertainty for all data points. The potential parameters obtained from Coulomb-modified eikonal model fit to the data are listed in table I. The calculated differential cross sections for the elastic scattering of ^{16}O + ^{16}O system at E_{lab}= 704 MeV are presented in Fig. 1 together with the observed data [3]. In this figure, the solid and dashed curves are the calculated results by the nuclear eikonal phase shift with the relative tangential velocity and asymptotic velocity at r_c, respectively. We can see in this figure that two calculated angular distributions are nearly identical at forward angles but are qualitatively different at large angles. From the descriptions of the elastic scattering data by the Coulomb-modified eikonal model using the tangential velocity at r_c shown in Fig.1, we found that our calculation provide reasonable fits to the refractive structure of the cross section at large angles compared with one by using asymptotic velocity. The reasonable χ^2/N value is obtained as listed in table II. It can further be seen in table II that the reaction cross section obtained from the phase shift using tangential velocity at $r = r_c$ give some larger value compared to the result using asymptotic velocity, due to the tangential velocity correction at r_c.

In figure 2, we plot the real (S_{RE}) and imaginary (S_{IM}) parts of the terms, $\frac{1}{i}(L + \frac{1}{2}) \exp(2i\sigma_L)(S_L^N - 1)$, as a function of angular momentum L, along with the partial reaction cross section σ_L. The S_{RE} and S_{IM}, in Fig.2(a), present the partial wave contributions to the cross sections in terms of orbital angular momentum L. In Fig. 2(b), we found that the value of the partial wave reaction cross section increases linearly up to L= 66. Beyond this L value, the partial reaction cross section decrease quardratically. The strong

TABLE I: Parameters of the fitted Woods-Saxon squared potential from the Coulomb-modified eikonal model using a tangential velocity at r_c, for ^{16}O + ^{16}O system at E_{lab} = 704 MeV.

V_o(MeV)	r_v(fm)	a_v(fm)	W_o(MeV)	r_w(fm)	a_w(fm)
242	0.926	1.349	48.7	1.189	0.961

TABLE II: Strong absorption radii (R_s), reaction cross sections (σ_R) and χ^2/N values from the Coulomb-modified eikonal model using a tangential velocity at r_c, for ^{16}O + ^{16}O system at E_{lab} = 704 MeV. 10 % error bars are adopted to obtain χ^2/N values.

R_s(fm)	$\sigma_{R_s}(mb)$	$\sigma_R(mb)^a$	$\sigma_R(mb)$	χ^{2a}/N	χ^2/N
6.76	1437	1476	1482	9.12	6.67

[a] Results from the Coulomb-modified eikonal model using a asymptotic velocity at r_c

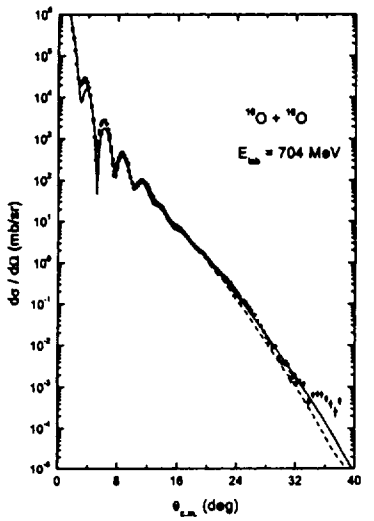

FIG. 1: Elastic scattering angular distributions for $^{16}O + ^{16}O$ system at $E_{lab} = 704$ MeV. The solid circles denote the observed data taken from Bartnizky *et al.* [3]. The dashed curve is the calculated result obtained from the Coulomb-modified eikonal model using a asymptotic velocity at $r = r_c$, while the solid curve is the one using a tangential velocity at $r = r_c$.

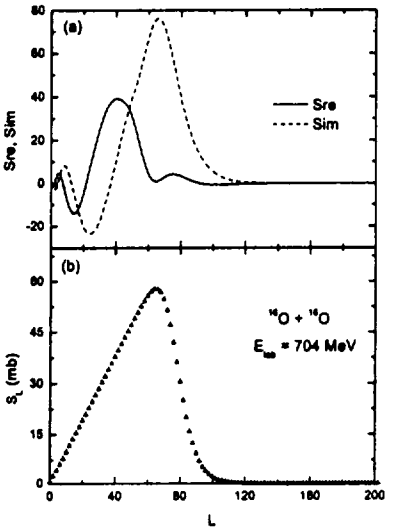

FIG. 2: (a) The real (S_{RE}) (solid curve) and imaginary (S_{IM}) (dashed curve) parts of the terms, $\frac{1}{2}(L+\frac{1}{2})\exp(2i\sigma_L)(S_L^N - 1)$, and (b) the partial reaction cross section σ_L.

absorption radius R_s in table I is defined as the distance for which $|S_L^N|^2 = 1/2$, i.e. the distance where the incident particle has the same probability to be absorbed as to be reflected. We can see that the strong absorption radius provides a good measurement of reaction cross section in terms of $\sigma_{R_s} = \pi R_s^2$.

In order to understand the nature of angular distributions for $^{16}O + ^{16}O$ system at E_{lab}= 704 MeV, the near- and far-side decompositions of the scattering amplitudes with the Coulomb-modified eikonal model using a tangential velocity at r_c were performed by following the Fuller's formalism [16]. The near-side amplitude represents contributions from waves deflected to the direction of θ on the near-side of the scattering center and the far-side amplitude represents contributions from the opposite, far-side of the scattering center to the same angle θ. The contribution of the near- and far-side components to the elastic scattering cross sections is shown in Fig.3 along with the differential cross sections. The differential cross section is not just a sum of the near- and far-side cross sections but contains the interference between the near- and far-side amplitudes as shown in Fig.3. This figure show near-side dominance from the long-range repulsive Coulomb interaction at forward angles and far-side dominance from the short-ranged attractive nuclear interaction at large angles. The Fraunhöfer diffraction pattern at intermediate angles in the elastic scattering cross section of $^{16}O + ^{16}O$ system at E_{lab}= 704 MeV is due to the interferences between the near- and far-side components. The magnitudes of the near- and far-side contributions are equal, crossing point, at $\theta = 4.7°$. However, the elastic scattering pattern at large angles is dominated by the refraction of the far-side trajectories.

Fig.4(a) show the real and imaginary parts of optical potential for $^{16}O + ^{16}O$ system

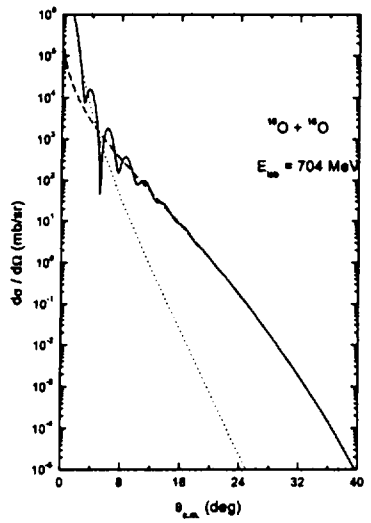

FIG. 3: Differential cross section (solid curve), near-side contribution (dotted curve), and far-side contribution (dashed curve) following the Fuller's formalism [16] from the Coulomb-modified eikonal model using a tangential velocity at $r = r_c$.

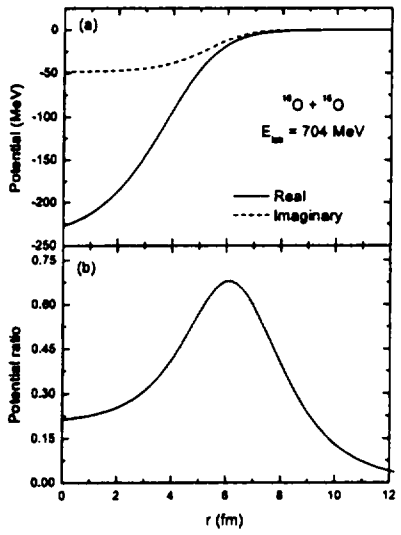

FIG. 4: (a) Real (solid curve) and imaginary (dashed curve) parts and (b) ratio of imaginary to real parts of optical potential for ^{16}O + ^{16}O system at E_{lab} = 704 MeV, respectively.

at E_{lab}= 704 MeV. The solid and dashed curves in Fig. 4(a) are the real and imaginary parts of optical potentials $U(r)$, respectively. As shown in this figure, the real potential is very strong compared to imaginary one. The strong real potential deflect internal trajectories to large negative angles, therefore, is required to describe the large angle behavior of cross sections corresponding to far-side scattering. The imaginary part of potential itself provides the radial weighting of flux removal from the entrance channel, and is consequently responsible for the absorption process in the nuclear reaction. The optical potential featuring a deep real one and a rather weak imaginary one leads to observe the contributions to the scattering from the interior region and allow refracted projectiles to populate the elastic channel and typical refractive phenomena could be observed in the angular distribution.

To investigate the features of optical potential systematically, we plot in Fig.4(b) the "reduced imaginary potential", $w(r) = W(r)/V(r)$, i.e., the ratio of the imaginary to real parts of the optical potential. The $w(r)$ curve shows remarkable for three characteristics. For small r values, $W(r)$ is very weak compared to $V(r)$ over the small r range, particularly, $W(0)/V(0) \sim 0.21$. This implies deep, elastic interpenetration of the target and projectile, and a feature unambiguously required by the appearance of refractive phenomena in the angular distributions. The large angle behavior of cross section is sensitive to the real optical potential over a wide radial region from the nuclear surface towards the interior. As a result the projectile ion can penetrate the nuclear surface barrier of the target, and the cross section becomes sensitive to the value of the real potential in the central region. In the large r range, both $V(r)$ and $W(r)$ have exponential tails, with quite different decay lengths with $a_v > a_w$. On the other hand, in the near surface, the pronounced maximum in $w(r)$ with a peak

value $\sim$ 0.68 occurs. The location of maximum seems to exist less than the "strong absorption radius", R_s, larger than R_w.

IV. CONCLUDING REMARKS

In this paper, we have analyzed the elastic scatterings of $^{16}O + ^{16}O$ system at E_{lab}= 704 MeV by the Coulomb-modified eikonal phase shift using a tangential velocity at the point of closest approach, r_c. The calculations gave a reasonably good agreements with observed data in this system. The value of the partial wave reaction cross section increases linearly up to L= 66. Beyond this L value, the partial reaction cross section decreases quardratically. It can be seen that the total reaction cross section calculated from the Coulomb-modified eikonal phase using a tangential velocity at r_c gave a some large value compared to the result using the asymptotic velocity. Through near- and far-side decompositions of the cross section for $^{16}O + ^{16}O$ system, we have shown that near-side dominate at forward angles, and the Fraunhöfer oscillations at intermediate angles are due to the interference between the near- and far-side amplitude. The elastic scattering pattern at large angles was dominated by the refraction of the far-side trajectories.

The present analysis for the $^{16}O + ^{16}O$ system at E_{lab}= 704 MeV has resulted in the optical potential featuring a deep real potential associated with a rather weak imaginary one. These strongly real and weakly imaginary potential values lead to near-transparency for the contributions to the scattering from the interior region and allow refracted projectiles to populate the elastic channel and typical refractive phenomena could be observed in the angular distribution. The ratio of imaginary to real parts of the potential, $W(r)/V(r)$, is found to be 0.21 at r=0. As a result, the projectile ion can penetrate the nuclear surface barrier of the target and the cross section becomes sensitive to the value of the real potential in the central region. We can see that the refractive part, dominated by the far-side component of the scattering amplitude, are sensitive to the real heavy-ion optical potential at small radii.

[1] E. Stiliaris, H. G. Bohlen, P. Fröbrich, B. Gebauer, D. Kolbert, W. von Oertzen, M. Wilpert and Th. Wilpert, Phys. Lett. **223**, 291 (1989).

[2] D. T. Khoa, W.von Oertzen, H. G. Bohlen, G. Bartnitzky, H. Clement, Y. Sugiyama, B. Gebauer, A. N. Ostrowski, Th. Wilpert and C. Langner, Phys. Rev. Lett. **74**, 34 (1995).

[3] G. Bartnitzky, A. Blazevic, H. G. Bohlen, J. M. Casandjian, M. Chartier, H. Clement, B. Gebauer, A. Gillibert, Th. Kirchner, Dao T. Khoa, A. Lepine-Szily, W. Mittig, W. von Oertzen, A. N. Ostrowski, P. Roussel-Chomaz, J. Siegler, M. Wilpert, Th. Wilpert, Phys. Lett. B **365**, 23 (1996).

[4] Dao T. Khoa, W. von Oertzen, H. G. Bohlen and F. Nuoffer, Nucl. Phys. **A672**, 387 (2000).

[5] M. P. Nicoli, F. Haas, R. M. Freeman, N. Aissaoui, C. Beck, A. Elanique, R. Nouicer, A. Morsad, S. Szilner, Z. Basrak, M. E. Brandan, and G. R. Satchler, Phys. Rev. **C60** 064608 (1999).

[6] T. W. Donnelly, J. Dubach and J. D. Walecka, Nucl. Phys. Nucl. Phys. **A232**, 355 (1974).

[7] C. K. Chan, P. Suebka and P. Lu P, Phys. Rev. C **24**, 2035 (1981).

[8] R. da Silveira and Ch. Leclercq-Willain, J. Phys. G **13**, 149 (1987).

[9] G. Fäldt, A. Ingemarsson and J. Mahalanabis, Phys. Rev. C **46**, 1974 (1992).

[10] F. Carstoiu and R. J. Lombard, Phys. Rev. C **48** 830 (1993).

[11] S. M. Eliseev and K. M. Hanna, Phys. Rev. **C56**, 554 (1997).

[12] C. E. Aguiar, F. Zardi, and A. Vitturi, Phys. Rev. **C56**, 1511 (1997).

[13] M. H. Cha and Y. J. Kim, Phys. Rev. **C51**, 212 (1995).

[14] Y. J. Kim and M. H. Cha, Int. J. Mod. Phys. **E10**, 373 (2001).

[15] D. M. Brink, *Semi-Classical Methods for Nucleus-Nucleus Scattering* (Cambridge Univ. Press, Cambridge, 1985), p.37.

[16] R. C. Fuller, Phys. Rev. **C12**, 1561 (1975).

접선속도 보정을 이용한 E_{lab} = 704 MeV 에서의 ^{16}O + ^{16}O 탄성산란에 대한 Eikonal 위상이동 분석

김 용 주
제주대학교 물리학과

최근접 거리에서 접선속도를 이용한 쿨롱-수정된 Eikonal 위상이동에 기초하여 E_{lab} = 704 MeV 에서의 ^{16}O + ^{16}O 굴절성 탄성산란을 분석하였다. 접선속도를 도입한 계산결과는 굴절성 각분포 패턴의 실험데이터를 성공적으로 재현할 수 있었다. 탄성산란 각분포에서 관측되는 Fraunhöfer 진동은 근측과 원측 진폭들의 간섭현상으로 설명할 수 있었다. E_{lab} = 704 MeV 에서의 ^{16}O + ^{16}O 굴절성 탄성산란을 기술하기 위해서는 강한 실수 퍼텐셜과 약한 허수 퍼텐셜이 요구되었다. 원측 진폭에 의해 지배받는 굴절성 부분은 작은 반경에서의 실수 퍼텐셜에 매우 민감함을 알 수 있었다.